Array Configuration: Design Description

020.23.00.00.00-002-DSN

Status: **RELEASED**

PREPARED BY	ORGANIZATION	DATE
C. Carilli, V. Rosero, B. Mason, B. Butler, J. Carilli, J. Wrobel, C. Walker	Configuration Working Group, NRAO	2022-08-31
E. Murphy	ngVLA/NM-Ops, NRAO	

APPROVALS	ORGANIZATION	SIGNATURES
E. Murphy, Project Scientist	ngVLA, NRAO	E. J. Murphy E. J. Murphy (Sep 1, 2022 13:59 EDT)
Thomas Kusel Systems Engineer	ngVLA, NRAO	Thomas Kusel (Sep 5, 2022 21:16 GMT+2)
R. Selina, Project Engineer	ngVLA, NRAO	R. Selina R. Selina (Sep 6, 2022 17:56 MDT)
W. Esterhuyse, Antenna Project Manager	ngVLA, NRAO	

RELEASED BY	ORGANIZATION	SIGNATURE
W. Esterhuyse, Antenna Project Manager	ngVLA, NRAO	

Change Record

Version	Date	Author	Affected Section(s)	Reason
A	2019-07-09	Lear	All	Initial Release
A.01	2021-09-30	All	All	Major updates for Revision D; see ngVLA Memos 82 and 92 for details.
A.02	2022-01-12	Lear	All	Formatting, minor copy edits.
B	2022-01-13	Lear	All	Prepared PDF for signatures and release.
C	2022-08-31	Carilli	All	Updated per CDR-T RIDS

Table of Contents

1 Introduction

1.1 Purpose

This document describes the ngVLA Array Configuration, Revision D. It covers the design approach, predicted performance, and risks associated with the design. This document will form part of the submission of the ngVLA Conceptual Design documentation package.

1.2 Scope

The scope of this document covers the design of the array configuration, specifically, the configuration design and its key constituents. It does not include specific technical requirements, which are addressed separately in [AD04].

2 Related Documents and Drawings

2.1 Applicable Documents

The following documents inform this conceptual design:

Ref. No.	Document Title	Rev/Doc. No.
AD01	Science Requirements	020.10.15.00.00-0001-REQ
AD02	System Requirements	020.10.15.10.00-0003-REQ
AD03	Operations Concept	020.10.05.00.00-0002-PLA
AD04	Array Configuration Technical Requirements	020.23.00.00.00-0001-REQ

2.2 Reference Documents

The configuration design draws extensively from work presented in the ngVLA memo series, available on the ngVLA Memo Series Web page. We refer the reader to these memos for more details on science simulations that relate to the configuration design and characterization of the design. Along with the ngVLA science book, *Science with the Next-Generation Very Large Array* (2018, ASP), these memos provide much of the provenance for the current configuration design in terms of scientific analysis and simulation verifying performance in key science areas[1].

The following documents provide additional supporting analysis or context that informed the design of the array configuration:

[1] Science imaging simulations can be found in memos: high redshift molecular gas (41, 44, 50, 83), proto-planetary disks and movies of planet formation (57, 68, 88), high dynamic range imaging of complex objects (memos 64, 67, 86), large scale structure in the Milky Way and nearby Galaxies (Memos. 54, 67, 89), continuum deep fields (31, 35, 44), locating fast transients (Memo 77), Quasar SZ imaging (Memo 80), imaging stellar photospheres and movies of mass loss from AGB stars (Memo 95), as well as in the chapters in 'Science with the next generation Very Large Array', 2018, ASP.

Ref. No.	Document Title	Rev/Doc. No.
RD01	ngVLA Science Use Case Parameterization Spread Sheet	2017-06-20 V24
RD02	ngVLA Reference Design Development & Performance Estimates	ngVLA Memo 17
RD03	Summary of the Science Use Case Analysis	ngVLA Memo 18
RD04	Key Science Goals for the Next Generation Very Large Array (ngVLA): Report from the ngVLA Science Advisory Council	ngVLA Memo 19
RD05	Image Capabilities: High Redshift CO	ngVLA Memo 13
RD06	Investigating the Early Evolution of Planetary Systems with ALMA and the Next Generation Very Large Array	ngVLA Memo 33
RD07	More on Synthesized Beams and Sensitivity	ngVLA Memo 16
RD08	ngVLA Dynamic Range	ngVLA Memo 30
RD09	Deep Fields at 8GHz	ngVLA Memo 35
RD10	Initial Imaging Tests of the Spiral Configuration	ngVLA Memo 41
RD11	Resolution and Sensitivity of ngVLA-revB	ngVLA Memo 47
RD12	The ngVLA Short Baseline Array	ngVLA Memo 43
RD13	Fast Switching Phase Calibration at 3mm at the VLA Site	ngVLA Memo 1
RD14	Possible Configurations for the ngVLA	ngVLA Memo 3
RD15	Snapshot coverage of the ngVLA: an alternate configuration	ngVLA Memo 49
RD16	Taperability study for the ngVLA and performance estimates	ngVLA Memo 55
RD17	High Dynamic Range Imaging	ngVLA Memo 64
RD18	Demonstrations and Analysis of ngVLA core + Short Baseline Array for Extended Structure Imaging	ngVLA Memo 67
RD19	A Study of ngVLA Subarray Efficiency: Plains and Fractions of the Core	ngVLA Memo 72
RD20	Subarray Selection for the Reference Observing Program	ngVLA Memo 76
RD21	Configuration: Reference Design Rev C.01 Description	ngVLA Memo 82
RD22	The ngVLA Long Baseline Array: Configuration Suggestions	ngVLA Memo 84

Ref. No.	Document Title	Rev/Doc. No.
RD23	Comparison of Alternative Configurations for the ngVLA Plains Subarray	ngVLA Memo 85
RD24	Imaging Evaluation of Two Mid Configurations	ngVLA Memo 86
RD25	Image Fidelity Study of KSG3	ngVLA Memo 89
RD26	Configuration: Reference Design Rev D Description	ngVLA Memo 92
RD27	Preliminary ngVLA Observing Band Availability Estimate	ngVLA Memo 73
RD28	Seismic study and risk assessment for ngVLA sites	ngVLA Memo 93
RD29	Surface Weather and Atmospheric Measurements at the VLA Site, VLBA Sites, and Relevant Locations in the Southwest US	ngVLA Memo 94 (in prep)
RD30	Evaluation of the Revision D array configuration for stellar imaging	ngVLA Memo 95

3 Subsystem Overview

The antenna configuration is a basic property of the array. It is an abstraction, defining the locations of antennas within the array. The cost of the antennas and supporting infrastructure is included within other packages of the conceptual design.

The longest baselines set the highest angular resolution of the array, while the shortest determine the largest-scale structures that can be imaged. The antenna distribution then sets the sensitivity as a function of spatial resolution and the shape of the synthesized beam (point spread function), as determined by weighting of the (u,v)-data.

The array will not be reconfigurable, yet it must perform a broad range of science programs with a wide range in spatial resolutions as a function of frequency, as summarized in ngVLA Memo 18 and in chapter 1 of *Science with the Next-Generation Very Large Array*. To perform this broad range of science programs, the array configuration design requires essential capabilities such as[2]:

- Ultra-high-resolution imaging of 1 pc-scale structures in distant radio jet sources associated with supermassive black holes (0.3 mas resolution at 1 cm wavelength).
- High-resolution, high-sensitivity observations of exoplanets forming on 1 AU-scales (7 mas resolution at 1 cm).
- High surface brightness sensitivity of 1 kpc-scale structures in the molecular gas in high redshift galaxies (100 mas resolution at 1 cm).

[2] Quoted resolutions and wavelengths are representative, not exclusive.

- High surface brightness sensitivity at arc-second resolution for imaging of tens of parsec-scale structures in nearby galaxies in line and continuum emission over a broad range in frequency.
- High dynamic range imaging (up to 10^5) at resolutions from 100 mas to arcsecond scales, for imaging complex radio continuum sources and deep fields over a broad range in frequency.

The configuration design reflects the multi-scale demand on the array science case. The sensitivity as a function of resolution will depend on the specific synthesized beam for the science application in question. As a guiding principle, we have adopted the goal of roughly a factor two loss in sensitivity relative to natural weighting, for spatial resolutions ranging from ~0.3 mas to 1000 mas at 30 GHz. The array performance for several key science programs has been documented in the memo series, as listed in the reference documents above.

4 Site Quality

Locating the majority of antennas in the Main Interferometric Array in the Southwest US and Mexico allows for maximum visibility of the southern sky from the Continental US. The high, dry plains in this area are well suited for observations up to 116 GHz due to generally high elevations (typical elevations of 1500 meters or higher) and low water vapor content. Figure 1 (on the next page) shows an example of the phase stability at the VLA site for observations at 90 GHz. These measurements show that using fast switching calibration provides acceptable calibration results (ϕ_{rms}< 40°) for observations at day or night during most of the year [RD13].

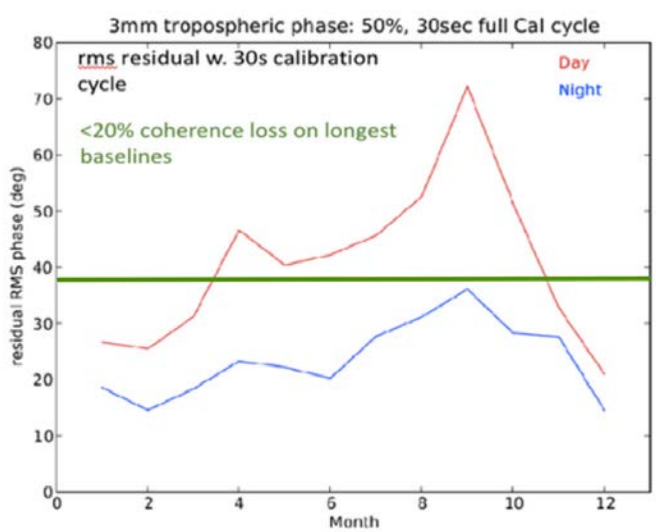

Figure 1: RMS phase residuals after fast switching calibration predicted for the VLA site at 90 GHz based on decades of phase monitoring with the Atmospheric Phase Interferometer (after [RD13]).

As a specific test of whether the location of the array would be suitable for 90 GHz observations, we have done a detailed analysis of what star forming molecular clouds could be observed to satisfy the needs of KSG1 [AD01], given known weather and other assumptions. We assume that the VLA is a good proxy for weather conditions over enough of the array that the results of [RD27] can be used. This should be true for the antennas situated in the Southwest US and Mexico. We use reasonable assumptions regarding calibration overheads. And we use the specific locations on the sky of six nearby star formation regions

(Perseus, LkHα 101, Taurus, Orion, Serpens/Aquila, and Cepheus). The results imply a lower limit of roughly 12% of time per year could be devoted to KSG1. Table 1 shows the amount of time per month that is available to observe KSG1. This is a lower limit because we have not included every possible star forming region in this analysis, but a restricted sample of six. If we included more star formation regions the value would go up, because they would cover the sky more completely, so fill in some ranges of time that are not covered in the current analysis. We do note that every star formation region has hundreds of potential targets that could satisfy the needs of KSG1. Note that even if we restrict this to just the Taurus star formation region, 5.4% of time could be devoted to KSG1, which is far more than is needed to complete the program (60 hours per year).

A calculation of atmospheric opacity at the VLA site (again, a proxy for much of the southwest), based on atmospheric models and weather statistics over a 10-year period, implies the 90 GHz opacity satisfies the '< 10% opacity more than 30% of the time' requirement throughout the year (requirement AAC0501).

A more complete analysis of weather statistics at the VLA site, Southwest US antenna locations, and VLBA sites and how that might affect potential high-frequency observing is forthcoming [RD29].

Month	Jan	Feb	Mar	Apr	May	Jun	Jul	Aug	Sep	Oct	Nov	Dec	All
Fraction (%)	20	12	11	9	12	11	4	3	7	14	20	19	12

Table 1: Fraction of time per month during which six nearby star formation regions (Perseus, LkHα 101, Taurus, Orion, Serpens/Aquila, and Cepheus) could be observed in Band 6-lower (70–90 GHz).

5 Array Configuration Design

5.1 Components of the Array Configuration

The range of angular scales to which the array must be sensitive cannot be accessed with any practical homogeneous array. A heterogeneous array is therefore required, consisting of three principal components (Figure 2; See ngVLA Memo 92 for further details on the Rev D configuration used for this review):

- Main Interferometric Array of 214 18m reflector antennas;
- Long Baseline Array (LBA) of 30 18m reflector antennas;
- Short Baseline Array (SBA) of 19 6m reflector antennas.

There will also be at least four 18m antennas equipped with instrumentation appropriate for accurate measurements of the total power in the antenna primary beam.

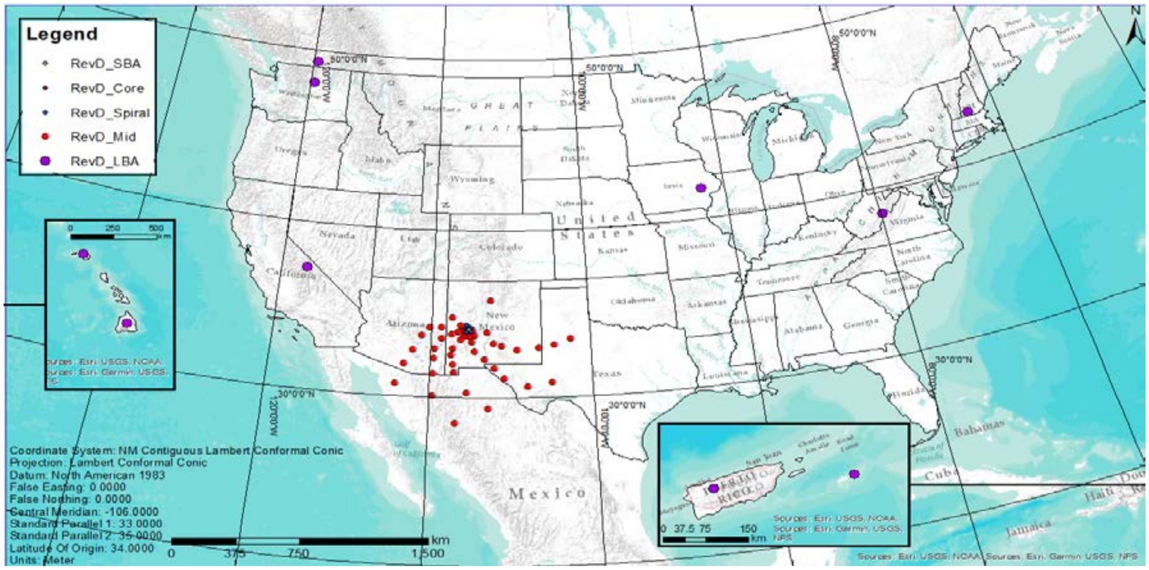

Figure 2: View of the LBA and Main Interferometric Array, with 244 18m antennas total. Each LBA site is denoted in purple and has 3 antennas. The legend lists sub-components of the Main Interferometric Array.

Table 2 summarizes the array configuration components. The design is practical, accounting for such logistic limitations as topography, utility access, local RFI sources, and land management/availability (see Section 6).

Component Name	Aperture Diameter (m)	Quantity	B_{min} (m)	B_{max} (m)
Long Baseline Array	18	30	130000 (38[3])	8794000
Main Interferometric Array	18	214	38	1068000
Short Baseline Array	6	19	10.9	60
Total Power/Single Dish	18	4[4]	--	--

Table 2: Summary of components within the ngVLA array configuration.

The Main Interferometric Array itself will have three spatially distinct antenna distributions, referred to as sub-components (Table 3; Figure 3, Figure 4, and Figure 5):

- Core Sub-Component: 114 18m antennas with minimum spacings of 38m (set by antenna design), distributed to a maximum radius of 2.2 km from the center of the Main Array;
- Spiral Sub-Component: 54 18m antennas distributed from a 2.3 km radius from the Main Array center to a maximum radius of 20 km;

[3] 38 m is the minimum baseline within an LBA site. 130 km is the minimum baseline between sites.

[4] The four total power antennas are a subset of the 214 antennas of the main array.

- Mid Sub-Component: 46 18m antennas distributed from a minimum radius of 26 km from the Main Array center to a maximum radius of 700 km.

Sub-Component	**Min. Baseline (m)**	**Max. Baseline (m)**	**Distribution Pattern**	**# Antennas**
Core	38	4269	Constrained random	114
Spiral	810	38995	5-arm spiral	54
Mid	17050	1068000	~5-arm spiral	46

Table 3: Sub-Components of the Main Interferometric Array.

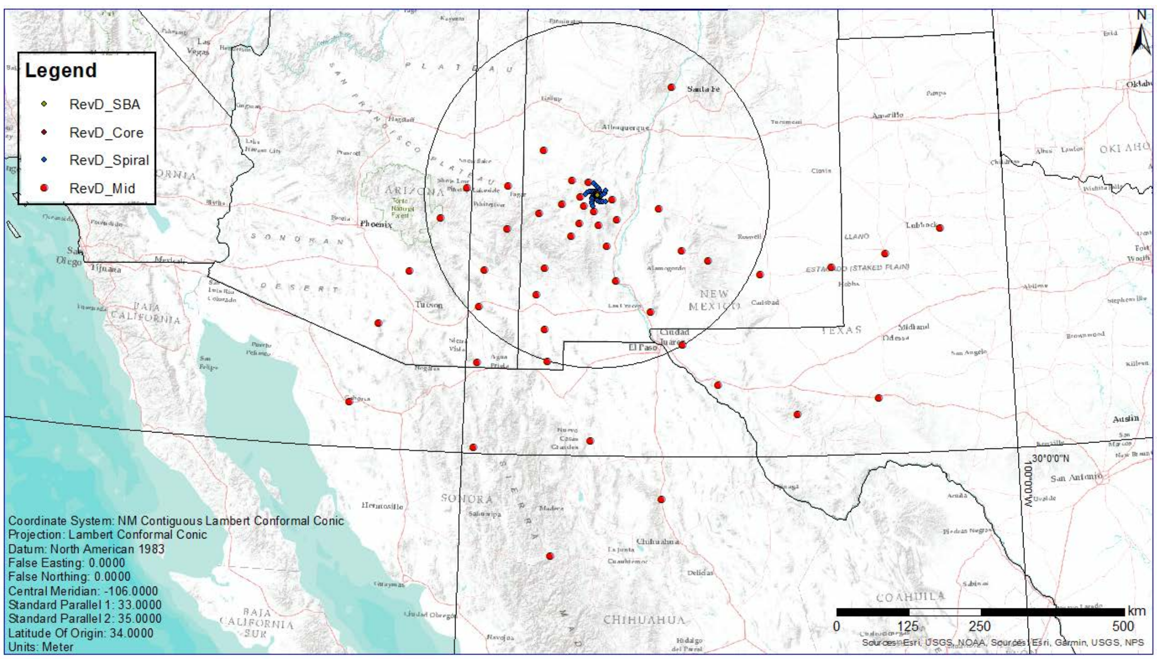

Figure 3: The Mid Sub-Component in the US Southwest and Mexico is shown as red circles. The Spiral Sub-Component is shown as blue circles at the center, for reference. The black open circle represents a 300 km radius around the center of the Main Interferometric Array. This buffer denotes the distance inside which the ngVLA is currently costing the laying of dark fiber solely for use by the project. Antennas outside the buffer would tie in to existing private company lines (ISP providers), which is also under investigation (see Long Haul Fiber Report, Doc No. 020.60.00.00.00-0002).

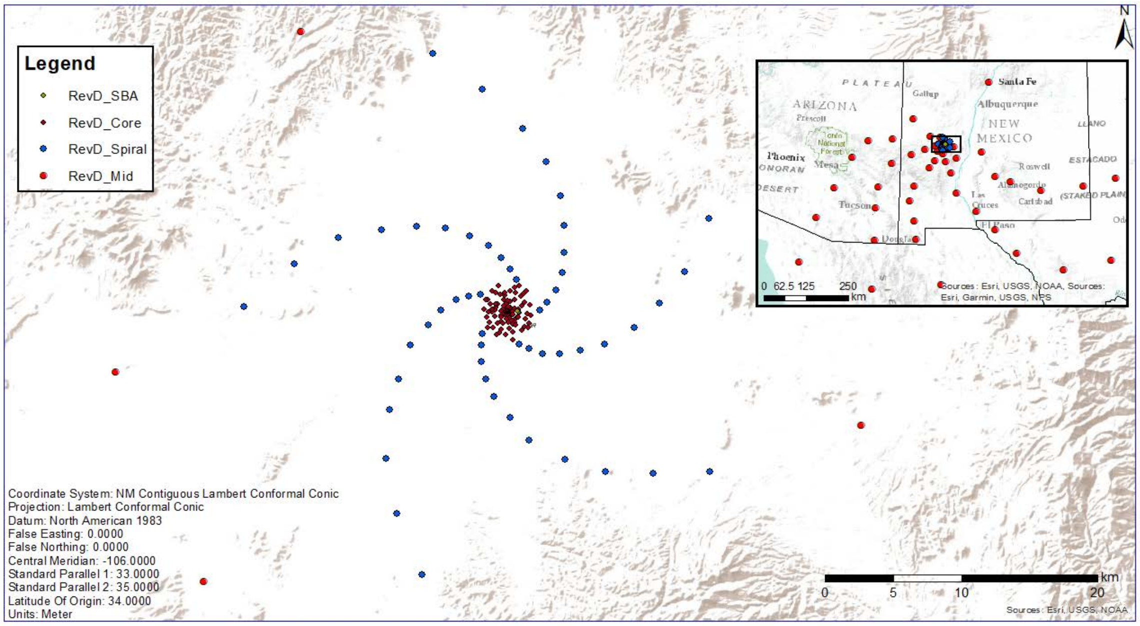

Figure 4: The blue circles are the antennas of the Spiral Sub-Component on the Plains of San Agustin in New Mexico. The red circles are the antennas of the Core Sub-Component. The lighter red circles show the relationship with the inner antennas of the Mid Sub-Component. The inset shows the relationship of the Spiral and Mid Sub-Components on larger scales.

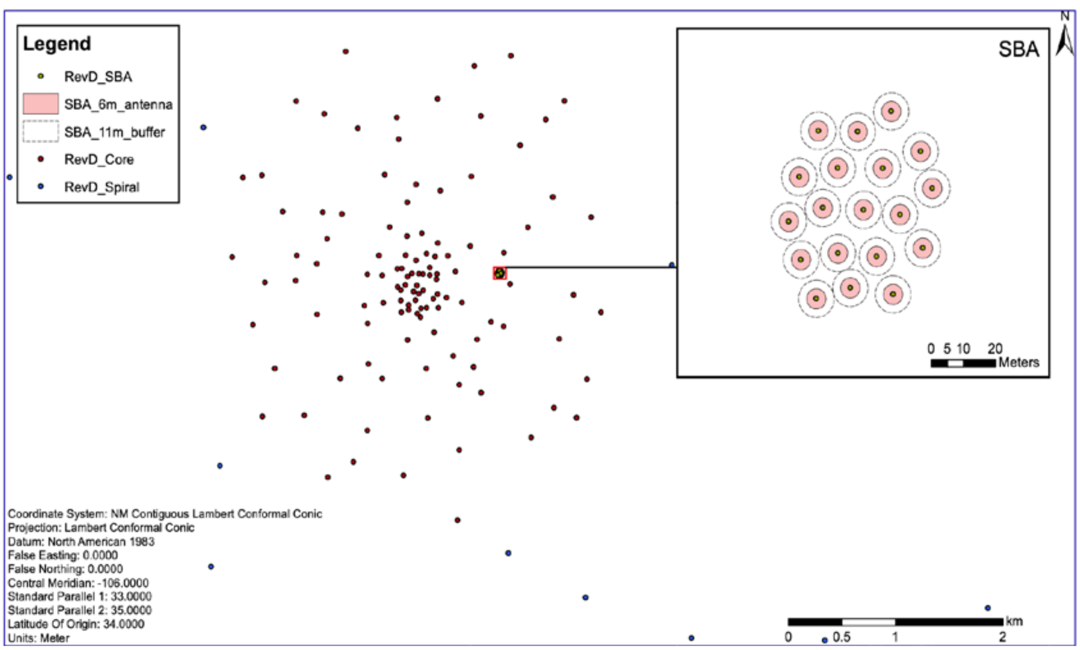

Figure 5: The Core Sub-Component (red circles) and the Short Baseline Array (overlapping grey circles), located near the center of the Spiral Sub-Component on the Plains of San Agustin. The inner antennas of the Spiral Sub-Component are shown as blue circles. The inset zooms in on the SBA, with dashed circles marking the 11 m safety diameters and pink circles marking the 6m antenna diameters.

5.2 Main Interferometric Array

We describe in more detail the Core, Spiral, and Mid Sub-Components of the Main Interferometric Array. We then consider the performance of the Main Interferometric Array in terms of noise and PSF quality with respect to UV-weighting. More detail on general imaging and taperability performance can be found in numerous ngVLA Memos, including 72, 76, 85, 86, 95, as well as memos related to specific science applications.

We expect that sub-arraying, meaning choosing antennas from different sub-components of the Main Interferometric Array to achieve a given scientific goal (e.g., the Spiral plus a few Core antennas to fill-in short spacings), will be employed frequently. The ngVLA is being designed such that science can be done with up to 10 sub-arrays commensally.

5.2.1 The Core Sub-Component

The antennas of the Core Sub-Component will be located at the current VLA site, in a centrally-concentrated, semi-random array, with minimum baselines of 38m (set by antenna design), to a maximum baseline of 4269 m (Figure 5). The configuration has been optimized to capture molecular line imaging programs for nearby galaxies, as given in KSG 3 (ngVLA Memo 89), and generally to perform high fidelity imaging for structures on scales of 0.1" to 1" at 100 GHz (see ngVLA Memos 67 and 92).

A detailed description of the genesis of the Core can be found in ngVLA Memo 92. In brief, the Core started with a random, but radially weighted[5] distribution of antennas. This gradual transition in aperture plane density between the outer spiral arms and the inner core provides more benign imaging characteristics than configurations with, for instance, a relatively discrete, dense core; while providing higher surface brightness sensitivity than configurations with no core at all. The initial pseudo-random array configuration was then run through the CONFI program in AIPS to reduce PSF sidelobes when using NA weighting. However, it was found that CONFI tended to move all the antennas to a ring-like distribution at the extremes of the configuration, thereby losing good short baseline coverage. Hence, CONFI was constrained to move only the antennas originally located beyond 600m from the center, and was stopped when a flat baseline distribution was obtained over a range of 100 m to 1300 m. A few antennas then had small position adjustments made to avoid structures or SBA antennas (see Section 6). The Core was then elongated by 10% in the North-South direction to obtain a rounder PSF at low and high declinations.

The snapshot UV-coverage and baseline distribution can be found in ngVLA Memo 92. Analysis of the PSF vs. UV-weighting can also be found in ngVLA Memo 92.

5.2.2 The Spiral Sub-Component

The Spiral Sub-Component consists of 54 18m antennas with baselines starting at a radius of 2.3 km, and extending to a 20 km radius (Figure 4). The antennas are distributed in a 5-arm spiral. The spacings along the arm are an exponential function, as defined in SKA Design Document WP3-050.020.000-R-002, and described in ngVLA Memo 82. We include a 10% of radius dither of each antenna to broaden the UV-distribution. The Spiral has been rotated to optimize public land usage, and individual antennas have been moved from obvious terrain or structure conflicts (see Section 6). The Spiral has also been elongated 10% North-South to improve the PSF at low and high declinations.

[5] Weighted toward more short baselines.

The snapshot UV-coverage and baseline distribution can be found in ngVLA Memo 92. A detailed analysis of a 5-arm spiral PSF vs. other configurations can be found in ngVLA Memo 41.

5.2.3 The Mid Sub-Component

The Mid Sub-Component consists of 46 18m antennas from 26 km to 700 km radius (Figure 3). The antennas are distributed along a rough 5-arm exponential spiral, extending predominantly toward the South, and taking into consideration terrain and other practicalities (see Section 4). There are 5 antennas in Mexico, 9 antennas in Arizona, and 6 in Texas. Included in Mid are the current VLBA sites at KP, LA, and FD. The Mid provides excellent UV-coverage for few mas-scale observations at 30 GHz to 100 GHz for proto-planetary disks, as well as providing excellent shorter baseline coverage for higher-resolution LBA imaging of complex objects.

The snapshot UV-coverage of Mid can be found in ngVLA Memo 92. Details of the genesis of the Mid configuration, and imaging performance relative to other antenna distributions, can be found in ngVLA Memos 49, 86, and 95.

5.3 Long Baseline Array

The Long Baseline Array is composed of 30 additional 18m antennas at ten different sites (Figure 2; Table 4). Clustering antennas at each site is a cost-effective way to increase the array's sensitivity while sharing the operations infrastructure per site. Clustering also allows unique science capabilities, including

- Simultaneous observations of the science target and the calibrator for paired-antenna phase calibration,
- Simultaneous frequency coverage across the same set of baselines for temporal-spectral variable source studies, and
- Use of sites individually, as small phased arrays for "single dish" observations, such as pulsar timing or fast transient searches.

The LBA by itself provides good UV-coverage on scales from a few hundred to 9000 km baselines, while incorporating the Mid Sub-Component fills in baselines to tens of km. For the outermost sites, the LBA has a second site within a few hundred km, to improve flux scale calibration (see ngVLA Memo 84).

The UV-coverage and baseline distribution of the LBA can be found in ngVLA Memo 92.

Antenna Quantity	Location	Notes
3	Puerto Rico	Arecibo Observatory
3	St. Croix	VLBA Site
3	Kauai, Hawaii	Kokee Park Geophysical Observatory
3	Hawaii, Hawaii	Not on Mauna Kea. New site.
3	Hancock, NH	VLBA Site

3	Green Bank, WV	GBO
3	Brewster, WA	VLBA Site
3	Penticton, BC	Dominion Radio Astrophysical Observatory
3	North Liberty, IA	VLBA Site
3	Owens Valley, CA	Owens Valley Radio Observatory

Table 4: Conceptual design antenna sites of the ngVLA Long Baseline Array.

5.4 ngVLA (Main+LBA) Performance

Figures 2–5 show the LBA and the Main Array's antenna distribution for each of its sub-components. This configuration has been designed to satisfy the broad requirements in resolution vs. sensitivity for the ngVLA science program. The distribution of baseline lengths for all 244 18m antennas included in the Main + LBA sub-components is shown in Figure 6. The consequence of having a relatively dense distribution of antennas on scales of a few km, then baselines extending to almost 9000 km, leads to a naturally weighted PSF for the 244 18m antenna distribution with three very different scales (see Figure 7):

- a narrow spike with high resolution (~0.3 mas at 30 GHz) due to the LBA antennas,
- a first skirt extending to 100 mas at 30 GHz at the 50% to 20% power level of the PSF due to the Spiral antennas,
- a second, broader skirt due to the Core antennas extending to 1000 mas at 30 GHz in the 20% to 10% power range.

The challenge for imaging is to optimize UV-data weighting to obtain a reasonable synthesized beam while maintaining sensitivity. For a reasonable synthesized beam, numerous numerical simulations have shown that high dynamic range imaging can be obtained by keeping the broad skirt to below 10% at a radius from the beam peak ~ FWHM of the PSF. ngVLA Memo 55 [RD16] describes the process of adjusting standard imaging parameters (Briggs weighting, UV-taper, cell and image size) to obtain an adequate synthesized beam shape for high quality imaging. The ngVLA project is performing a broader suite of simulations to quantify this metric, while algorithmic development is ongoing to optimize the imaging and science return for multi-scale arrays in general.

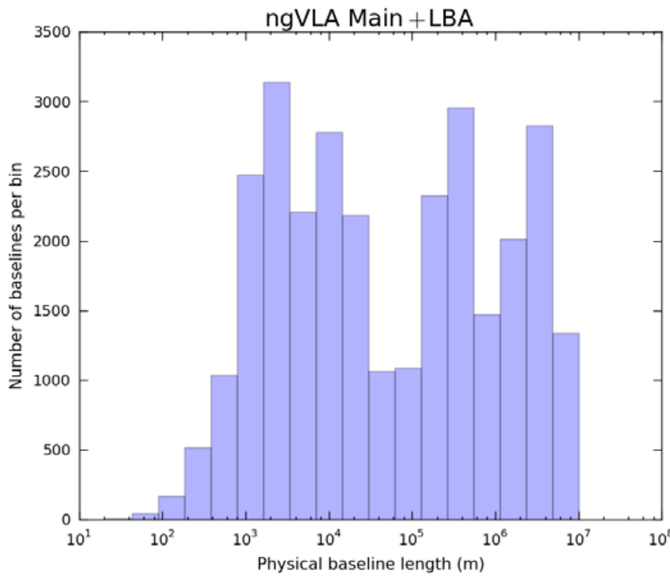

Figure 6: Number of baselines versus the baseline length for the 244 18-m antenna ngVLA (Main+LBA), using logarithmic bin sizes.

Image sensitivity will depend on the required resolution and imaging fidelity. Figure 7 and Figure 8 show the effects of adjusting UV-weights to obtain a target spatial resolution, while maintaining a PSF shape adequate for quality imaging [RD16]. These figures are based on a four-hour simulation at 30 GHz using the 244 18m antenna configuration, for a source at +24° declination observed during transit. The beam sizes reported in the caption of Figure 7 are the geometric mean of the major and minor full width at half maximum (FWHM) of the synthesized beam as parameterized by Gaussian fitting in the CASA tclean task.

To account for the sensitivity change due to use of UV-weights to obtain a quality PSF for imaging, we adopted an efficiency factor, η_{weight}, defined such that the image rms after weighting is: [η_{weight} x σ_{NA}], where σ_{NA} is the naturally weighted rms thermal noise. The process entails adjusting the taper and robust to obtain a well behaved PSF for a target spatial resolution (in particular, low skirt-levels), while optimizing sensitivity [RD16]. The gray points show the η_{weight} values for quality imaging at a target resolution. These values range between a factor 1.5 and 2.2 higher than NA weighting (red points), in the resolution range of 5 mas to 500 mas. We re-emphasize that the red symbols for NA weighting yield PSF shapes that have extremely broad skirts which preclude high-quality imaging (Figure 7).

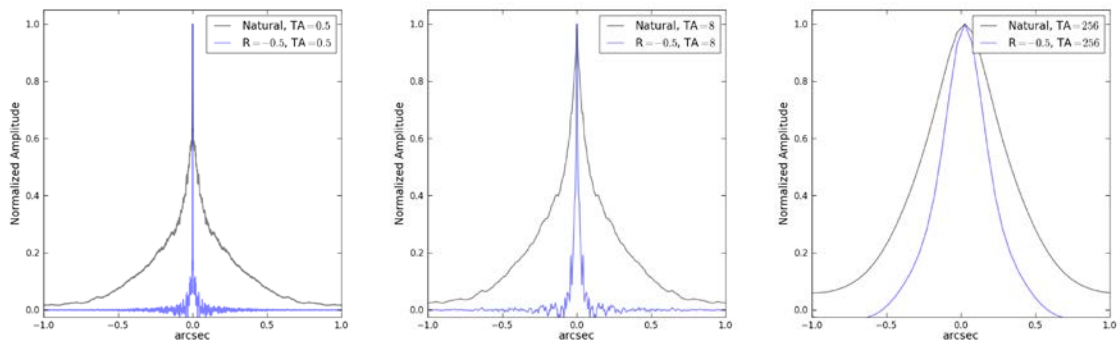

Figure 7: Simulated 30 GHz PSFs for the ngVLA configuration (Rev D, 244 18m antennas) over a range of resolutions, showing the effect of different imaging weights (TA: UV-taper in mas, R: Briggs robust parameter). The PSFs are a selection of the data presented in Figure 8. The FWHM of a Gaussian fit to the beams are, from left to right for the NA curves (black) are 2.3, 36.6, and 549 mas; the values for the Robust weighted curves are 1.4, 14.3, and 326 mas. These examples illustrate how combinations of robustness and tapering allow for a beam of much higher quality, i.e. greatly reduced beam skirts, but at the expense of sensitivity (see Figure 8).

Science simulations have verified that the current configuration and existing imaging tools in CASA, with appropriate weighting schemes, are adequate to perform the Key Science programs defined to date, such as imaging protoplanetary disks on scales down to 1 AU (Memos 57, 65 68, 88), CO in high redshift galaxies (Memos 41, 44, 50, 83), radio continuum deep fields (Memos 31, 35, 44), and large scale structures in nearby galaxies (Memos 54, 67, 89). Algorithmic studies of multi-scale information recovery with a heterogeneous array are a priority for the project in the coming year, which may improve performance beyond the current suite of imaging tools.

Several Python software tools have been developed in order to characterize the performance of the ngVLA, e.g., end-to-end pipelines that automate the process of creating and analyzing simulated observations for any given revision of the configuration reference design. For example, the *taperability* pipeline allows to compare different antenna configurations and the imaging performance pipeline allows the study of the requirements for the driving cases (e.g., PSF-level, image fidelity). Additionally, a Python command-line ngVLA sensitivity calculator is also available (https://gitlab.nrao.edu/vrosero).

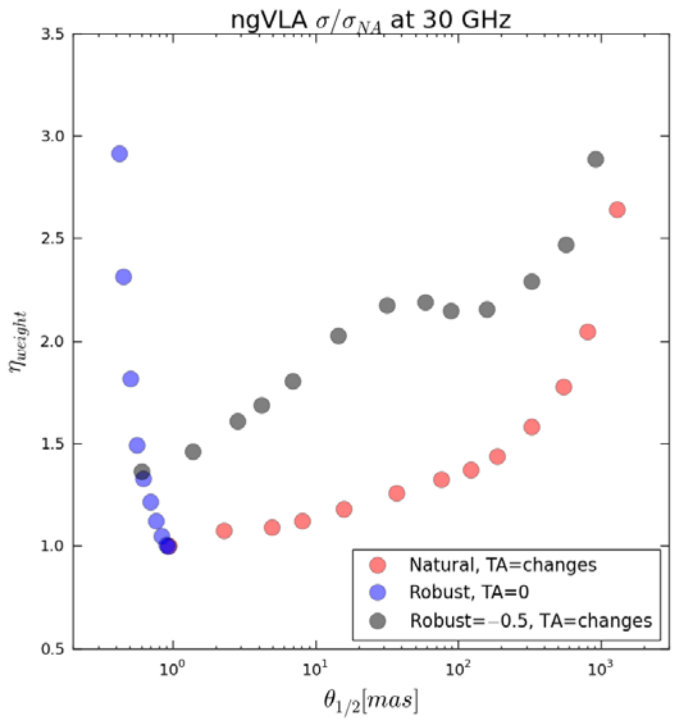

Figure 8: Image noise (rms) at different angular resolutions (FWHM) achieved by varying the imaging weights, simulated at 30 GHz using the 18-m 244 antenna configuration. The noise has been scaled relative to that of the naturally weighted image (σ_{NA}). The red symbols correspond to use of a UV-taper and natural weights, and the blue symbols to Briggs robust weighting without a taper. The gray symbols are for Briggs robust = –0.5 and a varying UV-taper, which is required to obtain a synthesized beam adequate for quality imaging (see Figure 7 and ngVLA Memo 55). For the blue points, the robust values go from -2 to +2 in steps of 0.4.

5.5 Short Baseline Array and Total Power Antennas

Due to mechanical clearance considerations, the ngVLA 18m antennas will not be able to be placed closer together than 38m. However, roughly 25% of identified science use cases require information on spacings shorter than this. In order to address this need, the ngVLA includes a short baseline array as well as a total power capability.

The ngVLA Short Baseline Array (SBA) consists of 19 6m antennas operated as an interferometer to fill spacings between 60 m and 11 m (Figure 5); basic design considerations are presented in ngVLA Memo 43. Spacings shorter still will be observed by the Total Power Antennas (TPA), a set of ~4 18m antennas capable of measuring total power accurately (see below). The SBA and TPA were designed to "feather" and/or be jointly deconvolved with observations from the Core Sub-Component of the Main Array, improving sensitivity to spatially large structures (up to 70 arcseconds at 90 GHz for the SBA alone, with TPA raster scans enabling recovery of much larger scales). The number and distribution of antennas in the SBA was selected to provide good surface brightness sensitivity, while also providing comparable surface brightness sensitivity to the shortest, overlapping baselines measured by the Core A histogram of the baseline lengths for the SBA and Rev.D core is shown in Figure 9. The integration time ratios needed to match the sensitivity of "adjacent" arrays (SBA:core and TPA:SBA) are shown in Table 5, computed using the same approach used by ALMA (ALMA Memo 598).

Simulations demonstrating the efficacy of the SBA and TPA are presented in ngVLA Memo 67. These memos used the previous (Rev.C) antenna configuration, which differs only in very minor respects from the current Rev.D SBA antenna configuration. The primary difference, as described in ngVLA Memo 82, is that the array orientation has been rotated by 30 degrees in order to reduce shadowing for low and high declination sources. For a 1hr 15min track on Sgr A* this rotation reduces shadow-flagged data by a factor of almost 5 down to only 6.4%. The locations of the SBA antennas have also been translated to a location in the Rev.D Core which is free of shadowing by 18m antennas. The SBA has been elongated North-South by 10% to improve PSF performance at low and high declinations.

Array 1, Array 2	T(Array 1) / T(Array 2)
SBA, Core	0.60
TPA (4 antennas), SBA	2.13

Table 5: Observing time ratios for the Rev.D ngVLA Core, SBA, and TPA. Times do not include observing overheads and thus represent ratios of integration time on the science target, and assume equal sky areas are observed. Ratios also implicitly assume that Array 2 is used at full natural-weight angular resolution.

Total Power Antennas: For purposes of Rev.D, it is provisionally assumed that *any ngVLA 18m antenna can function as a total power antenna.* The TPA would in this scenario be a flexibly allocated logical entity rather than a physically distinct set of antennas. This would allow more or fewer TP antennas as demand and weather conditions require. It is yet to be determined whether the distinctive requirements of total power observing will permit this flexibility in practice, or whether more specifically optimized hardware will be required for the TPA. An ngVLA Total Power Working Group (TPWG) has been charged with addressing this issue. The TPWG deliverables will inform the next iteration of the ngVLA design process leading up to the PDR.

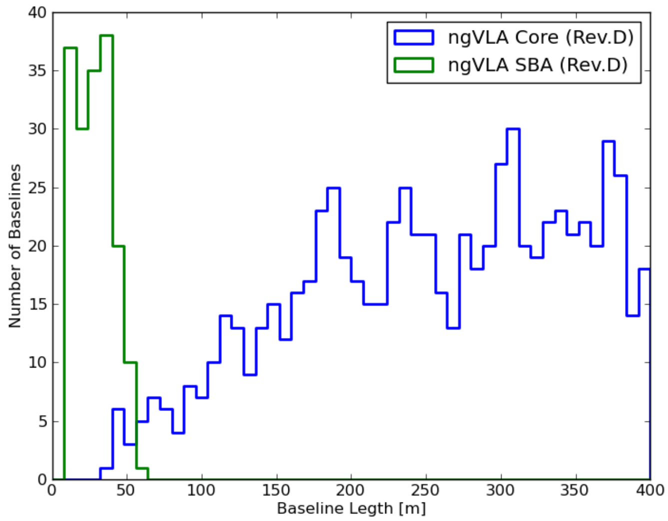

Figure 9: Histogram of baseline lengths for the Short Baseline Array (SBA) and the Rev.D Core Sub-Component. Note that Core baselines extend to 4,269m.

6 Practical Considerations for Antenna Locations

Antenna locations, in particular for the antennas outside the Plains of San Agustin, incorporate the practical considerations of land access, roads, power, fiber, interference environment, physical environment, safety, and security. Where possible, antennas have been placed on public land. Public land areas were chosen that are contiguous with nearby primary roads to allow convenient utility access and that are large enough to place the antenna some distance from the road to reduce the impact of radio frequency interference (RFI). In the case of the Spiral Sub-Component, an overall rotation and subsequent small shifts to antenna positions on the arms were made to prioritize placement on public lands. Of the 158 Spiral plus Core antennas on Plains of San Agustin, 15 are on private land.

Antennas have generally been placed within 1 km of existing primary roads to allow easier access to both utilities and service vehicles. Some access roads may require surface enhancement and improved drainage management. Sites were selected for several geographic features. In general, antenna sites are shielded by distance or terrain from easily identifiable RFI emitters such as urban centers, airports, radar installations, and large transmitter towers. Most antenna lines of sight are within ten degrees of the horizon. Sites were chosen to be outside visible flood boundaries and wetlands. In addition, sites were checked for potential landslide risk, specifically in areas affected by wildfires.

For antennas on the Plains of San Agustin, utilities can be accessed directly from those at the VLA site. The spiral form for the arms was chosen for the antennas on the Plains not only for imaging performance, but also for convenient emplacement of utilities. Each spiral arm can host utility trenches and access roads. Designs for electrical infrastructure provide power distribution systems that are redundant along each arm so that preventive maintenance (PM) or faults need not significantly affect UV coverage.

Costing and pathing are being investigated for dark fiber laid and owned by the NRAO in order to service the Mid Sub-Component antennas along the five arms, within 300km of the center of the array (see Figure 2). Antennas outside of this buffer, as well as the Los Alamos station, will be connected to existing public networks. Under this system, 30 of the 46 Mid antennas would be on NRAO-run fiber with 16 requiring tie-ins to private company fiber lines.

Many locations, including the Plains of San Agustin, and the proposed California and Mauna Kea ngVLA sites, are located on or near Quaternary fault zones. Using United States Geologic Survey studies, a general risk assessment has been made which can be read in more detail in ngVLA Memo 93, taking into account recent seismic activity, and a report which predicts the probability of peak horizontal surface movement over the next 50 years for Hawaii and the continental United States (USGS Open File Report 2008-1128). Based on USGS predictions, the most extreme peak horizontal spectral response acceleration (HSRA) is located in Mauna Kea, with a 10% probability of exceeding HSRA greater than 80% of gravity. The remaining sites, including the entire Plains, are located in areas with 10% probability of exceeding HSRA below 20% of gravity, meaning very low chance of damaging seismic activity (ngVLA Memo 93), as has been verified through 40 years of operation of the VLA. Experience with the pre-existing VLBA infrastructure on Mauna Kea shows that, despite the known potential for seismic activity on the Big Island, the region is a viable position for an ngVLA site. In general, all of the proposed sites are in well studied and highly monitored areas.

7 Future Work and Optimization

The Array Configuration is expected to go through additional iterations based on further testing and feedback. Likewise, we expect algorithmic developments may change the approach to multi-scale imaging in the future.

Some areas currently being explored are:

- Imaging simulations of the performance of the SBA and the LBA for their Key Science Programs.
- Multi-scale weighting: new algorithms for optimizing recovered information as a function of angular scale on complex celestial objects, for a multi-scale configuration such as that of the ngVLA.
- Multi-frequency synthesis simulations.
- Shortest LBA site-to-site baselines could be increased to ~ 500 km for better overall UV-coverage.
- Stagger the Spiral arm starting points to avoid resonances in the UV-coverage.
- Continued investigation of integrating fiber and utility data for costing.
- Continued investigation of terrain restrictions and RFI sources, in particular for outer Mid antennas, including Mexico and some LBA sites.
- Quantify site quality for sites at lower elevations.
- Smooth out depression in the Mid baseline histogram between 30 km and 100 km (Figure 6), by starting the Mid arms closer to the outer Spiral arms.

- Evaluate LAS for Rev.D subarrays (especially core); compute SB sensitivity as a function of taper for different subarrays.

8 Appendix

8.1 Abbreviations & Acronyms

Acronym	Description
AD	Applicable Document
AIPS	Astronomical Image Processing System
AU	Astronomical Unit
CASA	Common Astronomy Software Applications
FWHM	Full Width at Half Maximum
HRSA	Horizontal Spectral Response Acceleration
KSG	Key Science Goal
LBA	Long Baseline Array
M&C, M/C	Monitor and Control
NES	Near Earth Sensing
ngVLA	Next Generation VLA
NRAO	National Radio Astronomy Observatory
NSF	National Science Foundation
PM	Preventive Maintenance
PSF	Point Spread Function
RD	Reference Document
RFI	Radio Frequency Interference
SBA	Short Baseline Array
TBD	To Be Determined
TPA	Total Power Antenna
USGS	United States Geological Survey
VLA	Jansky Very Large Array

VLBA	Very Long Baseline Array
WVR	Water Vapor Radiometer

020.23.00.00.00-0002-DSN-ARRAY_CONFIG_DESIGN_DESCR.docx

Final Audit Report 2022-09-07

Created:	2022-09-01
By:	Alicia Kuhn (akuhn@nrao.edu)
Status:	Signed
Transaction ID:	CBJCHBCAABAASxVJfRVqu2LufFjxz_6V_WrKI0F1VrSy

"020.23.00.00.00-0002-DSN-ARRAY_CONFIG_DESIGN_DESCR.docx" History

- Document created by Alicia Kuhn (akuhn@nrao.edu)
  2022-09-01 - 5:48:20 PM GMT
- Document emailed to emurphy@nrao.edu for signature
  2022-09-01 - 5:49:07 PM GMT
- Email viewed by emurphy@nrao.edu
  2022-09-01 - 5:54:09 PM GMT
- Signer emurphy@nrao.edu entered name at signing as E. J. Murphy
  2022-09-01 - 5:59:05 PM GMT
- Document e-signed by E. J. Murphy (emurphy@nrao.edu)
  Signature Date: 2022-09-01 - 5:59:07 PM GMT - Time Source: server
- Document emailed to Thomas Kusel (tkusel@nrao.edu) for signature
  2022-09-01 - 5:59:09 PM GMT
- Email viewed by Thomas Kusel (tkusel@nrao.edu)
  2022-09-05 - 7:15:45 PM GMT
- Document e-signed by Thomas Kusel (tkusel@nrao.edu)
  Signature Date: 2022-09-05 - 7:16:07 PM GMT - Time Source: server
- Document emailed to rselina@nrao.edu for signature
  2022-09-05 - 7:16:09 PM GMT
- Email viewed by rselina@nrao.edu
  2022-09-05 - 7:45:45 PM GMT

Signer rselina@nrao.edu entered name at signing as R. Selina
2022-09-06 - 11:56:07 PM GMT

Document e-signed by R. Selina (rselina@nrao.edu)
Signature Date: 2022-09-06 - 11:56:09 PM GMT - Time Source: server

Document emailed to westerhu@nrao.edu for signature
2022-09-06 - 11:56:11 PM GMT

Email viewed by westerhu@nrao.edu
2022-09-07 - 7:10:54 AM GMT

Signer westerhu@nrao.edu entered name at signing as Willem Esterhuyse
2022-09-07 - 7:11:10 AM GMT

Document e-signed by Willem Esterhuyse (westerhu@nrao.edu)
Signature Date: 2022-09-07 - 7:11:12 AM GMT - Time Source: server

Agreement completed.
2022-09-07 - 7:11:12 AM GMT